

RECENT ADVANCES AND USES OF
NON DESTRUCTIVE TESTING

By

Dr. S. Ramaseshan
Jawaharlal Nehru Fellow

Keynote Address delivered at the Non-Destructive
Testing Seminar held on 28-29 June, 1979 organised by
NDE Centre, Central Laboratory, HAL(BC) Bangalore-560017

RECENT ADVANCES AND USES OF NON-DESTRUCTIVE TESTING

(KEY-NOTE ADDRESS)

By

S. Ramaseshan*

INTRODUCTION

I am indeed happy to give this talk at this Seminar on Non-Destructive Testing (NDT) organised by the Central Laboratory of Hindustan Aeronautics Limited. I am happier still to note the large number of Scientists and Engineers from various parts of India belonging to different organisations, laboratories and factories taking part in this Seminar.

Many experts will be speaking at this seminar on different aspects of NDT. It is not my intention to step on their toes and to cover the same ground. I have, therefore, decided to entertain you by showing a few slides on some exciting applications of NDT. I shall touch upon a few of the advances that have taken place in the field. Incidentally we will see that every new NDT technique that has been developed is based on at least one important fundamental discovery in science.

I hope that this talk provokes new thinking and research in NDT. It is also my fond desire that a large industry like H.A.L. will one day not only design planes but will also stimulate research in applied and pure science.

THE PILTDOWN MAN

At the end of the nineteenth century, many artefacts, human skeletons (like that of the Heidelberg Man) and cave paintings (as in Lascaux and Altamira) of the Paleolithic period were discovered in Continental Europe. The anthropological

*Jawaharlal Nehru Fellow, National Aeronautical Laboratory

establishment in Great Britain was, therefore, very despondent as no such findings were made there. At last in 1912, in the downs of Sussex, amongst the gravel, were found fauna, human artefacts, a skull bone and a mandible (jaw bone) lying close to each other. The skull and jaw bone were browned to the same extent - strongly suggesting that they belonged to the same animal. A reconstruction (Fig.1) of a new ape like human was made. The discovery was triumphantly announced at the meeting of the Geological Society of Great Britain in December 1912 by Charles Dawson the discoverer and Smith Woodward, the eminent anthropologist. The discovery of *Eoanthropus Dawsoni* or the Piltdown man as it was called, was greeted with great enthusiasm in Great Britain. It was thought that Darwin's famous missing link, the first human was an Englishman! Later discoveries of human remains in Africa made the position of the Piltdown Man rather anomalous. Four decades later in 1953, Kenneth Oakley had the brilliant idea of comparing the fluorine content of the skull bone and the mandible - which should have been the same if they belonged to the same age and had remained together in the same environment all these intervening years. The fluorine contents, were very different and proved beyond doubt that the two bones did not belong to the same individual. X-ray fluorescence analysis also showed the presence of potassium and chromium on the surface, establishing that a hoax had been perpetrated. The 'ageing' had obviously been achieved by dipping the specimens into potassium dichromate solutions! The mammalian fauna had also been planted in the gravel and the artefacts manufactured. The identification of the culprits presented many problems. The name of the renowned philosopher and anthropologist-Tailard de Chardin was for sometime associated with the fraud. But it is now fairly certain that the hoax was due to the Oxford anthropologist Professor William Sollas and was done to belittle (Sir Arthur) Smith Woodward, the keeper of the British Museum, for whom the former had, 'little liking'!

X-RAY FLUORESCENCE ANALYSIS

What is this x-ray fluorescence analysis? Moseley, the outstanding student of Lord Rutherford (who died in Gallipoli

in the First World War) mainly contributed to the development of this technique. When materials are bombarded by electrons (or hard x-rays) the electrons in the inner shells of the atoms are ejected. The subsequent filling up of the inner shells by electrons from the outer shells caused x-rays to be emitted. These are characteristic of the elements contained in the target (Fig.2).

The x-ray lines are much fewer than the atomic lines of optical spectroscopy where the electrons in the outer shells are involved. X-ray excitation is non-destructive, so that this /also method proves extremely convenient for elemental analysis. The wave length of the emitted x-rays can be determined by diffraction from a crystal (called an x-ray spectrometer or spectrograph). The wavelength can also be determined by measuring the energies of the emitted x-rays using a lithium drifted silicon crystal and a multichannel analyser. The wave lengths identify the element while the intensity (determined with respect to an internal standard) gives the quantity of the element present. These pioneering experiments led Moseley to the concept of the atomic number of elements which revolutionised chemistry and chemical physics.

Many improvements have been made in the X-ray spectrometer since Moseley's time. The x-ray microprobe analyser and the electron probe analyser in the scanning electron microscope are modern versions wherein a complete qualitative and quantitative elemental analysis over a micro-region can be carried out within a few minutes.

LIQUID AND GAS INCLUSION IN MINERALS

Much valuable information can be obtained on the geothermal history of the earth and the genesis of minerals by analysing the tiny bubbles of liquids or gases entrapped in a mineral specimen. How does one do it without letting out the liquid or gas? These

bubbles are usually only a few microns in diameter and the mass of the material to be analysed is less than 10^{-9} or 10^{-10} gm. Since these contain molecules, simple elemental analysis is not enough. All molecules vibrate and their vibrational frequencies ($\nu_1, \nu_2, \nu_3, \dots$) can be used to identify them. However, these vibrational frequencies appear in the far infrared region. In 1928 Raman discovered that the entire infrared spectrum can be shifted over to the visible region! If the molecules are illuminated by a monochromatic radiation the incident photon of frequency (ν_0) excites the vibrational frequencies and in this process loses energy, so that the scattered light has frequencies corresponding to $(\nu_0 - \nu_1)$, $(\nu_0 - \nu_2)$ and $(\nu_0 - \nu_3)$ (Fig.3). These spectral lines (known as the Raman lines) can be detected and recorded in a spectrograph. If the molecules are in the excited state and are vibrating, then the molecule can impart energy to the incident photon (ν_0) so that energy of the scattered photon is increased and the frequencies corresponding to $(\nu_0 + \nu_1)$, $(\nu_0 + \nu_2)$ and $(\nu_0 + \nu_3)$ appear on the more energetic side or the 'blue side' of the incident radiation. These are the 'antistokes Raman lines'. The Raman Spectrum is a thumb print of any molecule. Fig.4 shows the gas/liquid inclusion and their Raman spectra obtained by using Laser Raman Spectroscopy. In one case 4(a) the mixture consists of Methane and Carbon-dioxide ($\text{CH}_4 + \text{CO}_2 + \text{H}_2\text{S}$) in the proportion 66%, 33% and 1% while in the second (4b) the bubble is pure liquid CO_2 . The pressure inside the bubble is at least 33 atmospheres to liquify CO_2 at room temperature.

THE TURIN SHROUD

An object which is considered to be one of the most sacred relics in christendom and which is being examined by NDT specialists from all over the world is the Turin Shroud. This is a piece of linen (14 ft 3 inches x 3 ft 7 inches) on which the striking 'negative' image of a figure resembling that of Christ is imprinted (Fig.5).

It is not the effeminate figure of Christ of the

renaissance painters but a mere primitive vigorous one of the earlier painters of the 4th and 5th centuries. This cloth is reputed to be the shroud that wrapped the body of Jesus Christ after his crucifixion! There are marks on the back (scourge marks), stains near the forehead (the crown of thorns) and distinct black marks near the nailed wrist. How did the figure get imprinted? Was it painted or did it have some other origin?

Historically the shroud has been traced to Odessa in the 6th century, France in the 13th - 14th century and is now in Italy. Fine pollen grains have been collected from the shroud and analysed. There are pollens of 48 plants, 16 from plants in France and Italy, 9 from those near the Caspian sea (Odessa?) and 21 from saline desert plants (Israel Jerusalem?) Careful non-destructive analysis indicates that the so called blood stains do not have even traces of haemoglobin. Scientists are not certain whether traces of blood can be identified after 2000 years. The shroud has also been through two disastrous fires.

One theory is that the aloes and myrrh put along with a dead body may have chemically attacked the linen to produce the image. The surface of the fibres appear to be scorched (caused by the heat of resurrection say the believers!), the darkening differing from point to point producing the spectacular image. By microdensitometering the photograph and assuming the intensity to be directly proportional to the distance of the cloth from various parts of the body (Fig.6) a striking three dimensional image has been reconstructed (Fig.7). The authorities in charge of the shroud are permitting NDT scientists to examine and study the shroud provided care is taken to see that no damage is done. They have even given one long fibre from the shroud to be used for (destructive) carbon dating. A team of 30 NDT experts are now working on the shroud using every conceivable technique, - x-ray fluorescence analysis, thermography, optical fluorescence, infrared and ultra violet techniques, radiography etc to solve the nature of this mysterious image and its origin.

SEARCH FOR HIDDEN CHAMBERS IN THE PYRAMIDS

Do the pyramids of Egypt have secret chambers inside them? How could one x-ray these giant monuments having volume about $2.5 \times 10^5 \text{ m}^3$ and mass $3 \times 10^8 \text{ kg}$ and find out whether some priceless jewels and archaeologically important materials are not hidden in them? This was the question that Luis Alvarez the nuclear physicist asked himself a few years ago. There are some reasons to suspect the existence of secret chambers in these pyramids. The three great pyramids of Gizeh are situated a few miles southwest of Cairo, the two largest of those being Cheops (Base 230 m x 230 m and height 145 m) and Chephren (base 215.5 m x 215.5 m and height 145 m). This complexity of the internal architecture of pyramids increased during the Fourth Dynasty until the time of Cheops and then it gave way to quite simple designs. The simplicity of Chephren's pyramid compared to the elaborate structure of his father's great pyramid is explained by archeologists in terms of a "period of experimentation".

An alternative explanation for the sudden decrease in internal complexity could be (according to Alvarez) that Chephren architects had been more successful in hiding their upper chamber than were Cheops's. He evolved a technique of looking inside the pyramids using the penetrating cosmic ray muons which are continually bombarding us from outside. Alvarez used spark chamber detectors. The story of these measurements reads like a fairy tale. Scientific co-operation between USA and Egypt went on although there was complete break in the diplomatic relation between the two countries! Cosmic ray detectors with active areas of 4 m^2 and high angular resolution were installed in the chamber just below the base of the pyramid. The cosmic ray measurements and the subsequent computer calculations clearly showed the 4 diagonal ridges of the pyramid but the intensity definitely suggested that no chamber with volumes similar to the 4 chambers in the pyramid Cheops and that of his grand father Sneferus exist in the mass of limestone. This is perhaps the largest object that has been examined by NDT!

X-RADIOGRAPHY AND X-RAY TOMOGRAPHY

The principle used by Luis Alvarez for shadowing the massive pyramids employing the penetrating cosmic ray muons is the same as that of X-radiography. The discovery of x-rays by Wilhelm Rontgen in 1895 started the revolution in physics. What a great mind can do with a 'chance' discovery can be seen by reading Rontgens first paper which is remarkable in many respects. All of us have seen the famous radiograph taken by him of a left hand with a ring on its third finger (Fig.8). But we also know that in an X-radiograph the internal structures superpose so that bones will obscure the underlying structure. It has recently been possible to overcome this by a technique called the computer Tomographic X-ray scanning. In this the X-ray source and the detectors system move simultaneously around the object measuring the transmitted intensity (Fig.9). As many as a million intensity measurements are taken and recorded on tape and a computer processes the data and produces a picture (Fig.10). The basic principle of this method can be crudely understood in the following manner. If the object rotates about a particular axis all details except of those which lie exactly on the axis of rotation get smeared out. The computer actually reconstructs this eliminating the smeared data. The solution to this problem of course is very complex requiring mathematical and computational ingenuity. This remarkable instrument is now to be found in many hospitals and diagnostic centres. Its resolution is so good that it can actually distinguish between healthy tissue and diseased soft tissue.

NEUTRON RADIOGRAPHY

With the advent of nuclear reactors (and particle accelerators), Radiography using neutrons has become practical. To be most useful in radiography, neutrons must be slowed down and these "thermal neutrons" can be obtained directly from nuclear reactors. For the different elements of the periodic table the absorption characteristics of thermal neutrons and x-rays are

essentially reversed. Heavy elements like lead, bismuth and uranium which strongly absorb x-rays are practically transparent to thermal neutrons. Conversely, hydrogen, lithium, boron and other light elements strongly absorb thermal neutron while they allow x-ray to pass through them freely. There are however some heavier elements like cadmium, gadolinium, samarium and europium which absorb thermal neutrons rather strongly.

The complementary nature of x-rays and neutrons is illustrated by the radiography of an explosive pellet (Fig.14). The neutron radiograph shows shadows of the organic materials, the plastic cap and coating on the aluminium cap etc, while the x-radiograph shows shadows of the metallic components, and the lead based ~~mixed~~ explosives. Neutron radiography helps in the inspection of objects with materials containing hydrogen, like plastics, organic materials etc. Fig.12 illustrates how the efficiency of epoxy potting of electronic filters can be detected by neutron radiography. The testing of an epoxy bonded helicopter blade is illustrated in Fig.13. Turbine blades with cooling passages are cast. After casting, the ceramic cores have to be removed completely by leaching. A small residue of core can cause a hot spot and cause a "burn through". To detect this some Gd_2O_3 (which absorbs neutrons) is added to the ceramic forming the core. Fig.14 illustrates the inspection of these by neutrons.

Fig.15 shows how epoxy bonded aluminium honey combs can be tested for faults.

Fig.16 shows an 8th century Buddha statue of the Gupta period, neutron radiographed to determine how the statue was made.

LASER INDUCED SHOCK WAVES AND X-RAYS

The use of ultrasonics for flaw detection is well-known and this will be the subject of a few talks in this seminar. It is interesting that J.C. Bose one of India's outstanding

experimenters - renowned for his work on microwaves - studied the 'cry of metals' in the first decade of this century. His work is, in a sense, related to the modern acoustic emission which seems a promising method of monitoring fatigue. A high frequency ultrasound is emitted every time a micro crack forms in a metal.

Much progress has also been made in ultrasonic imaging, particularly in the field of medical technology. I shall always remember the relief on the face of my friend in Holland when ultrasonic imaging revealed that his wife was not going to have twins!

The discovery of the laser has been a boon to NDT. I am sure all of you noted that the Raman spectrum of 10^{-10} gm of gas in a mineral could be recorded in a few seconds only because of lasers. Raman in his original researches took a few days to record the Raman spectrum of gas!

There are many limitations to the conventional ultrasonic flaw detection technique. For example, it would be difficult to use it in the non-destructive testing of microwelds. In conventional techniques the pulse duration is 100 to 200 nano seconds (ns) which is much higher than that required to test thin sheets which requires 10 to 40 ns pulses. Pulses induced by lasers have these short durations. The absorption of laser radiation at the surface of a solid causes rapid heating. If the intensity is kept low enough not to melt the solid the heat absorbed by the thin layer increases its thermal energy. If the heating of the layer is faster than that conducted away into the bulk material, the heated layer expands and exerts a "stress pulse" on the material, i.e. an ultrasound shock wave of very high frequency is generated. Lasers using Yttrium Aluminum Garnet (YAG) (1.06μ wavelength with a pulse time of 15 to 17 ns and intensity 40 mj) are ideal for such experiments. Microprobes have been developed specifically to detect these pulses so that microwelds can be tested using this technique.

Lasers can be used to produce ultrasound of frequency 10^9 to 10^{10} Hertz. Since the wave length is only a few microns, extremely fine defects can be detected.

To me as an x-ray crystallographer one of the most exciting things that has happened (as a direct result of fusion research) is the generation of x-rays using lasers. Normally x-rays are generated by bombarding a target by fast electrons. The efficiency of x-ray production is less than 1% i.e. more than 99% of the energy gets converted to heat. When x-rays are generated by laser heating the conversion efficiency is as high as 25% - 40%. Further the pulses are so short (10 ns) that these x-rays can actually 'arrest' ~~in~~ a bumble bee in flight. The physics of this high efficiency can be understood in the following manner. The coherent laser radiation can be focussed to a very small area to make the energy density very high. The pulsing is such that the metal evaporates and forms a plasma. The electrons of the plasma are accelerated by the intense electric field to emit x-rays by the 'Brehmstrahlung' process. The electrons also collide with the atoms and ions of the metal in the plasma to emit x-ray. The metal solidifies as soon as the laser pulse stops.

Lasers can also be used to produce neutrons. But the intensity of the neutrons so produced is still low. But a considerable improvement is expected in the next five years.

HOLOGRAPHY

Holography is a photographic process which allows a three dimensional record to be made of an object or a scene. Fig.17(a) illustrates the optical arrangement used in taking an ordinary photograph. A white light source illuminates an object. A lens collects the reflected light and produces an amplitude (or intensity) record of the light distribution on the photographic material giving the usual two dimensional photograph. In holography Fig.17b, the object is illuminated by coherent laser light.

The photographic plate receives light simultaneously from (a) the object and (b) the source laser (the latter by reflection from a mirror). The two wave fronts interfere and the interference pattern is recorded. This plate contains information not only about the light distribution reflected by the object but also the phase information from which the shape and the position of the object can be reconstructed. This is done by viewing the hologram again by laser light Fig.17c. A virtual three dimensional image which is identical in all respects to the original object can be seen.

If after processing, the hologram is replaced in its initial position and the object is deformed in some way to alter its shape, the two images will no longer coincide. This lack of coincidence results in the object appearing to have a fringe pattern covering it; and each fringe contour is basically equal to a change in shape of the original object by half a wave length (Fig.18a). Hence, an accurate mapping of the deformation is possible. Fig.18b shows the use of holography in examining crack propagation while Fig.18c shows how holography can be used to detect subsurface faults. The strength of a honeycomb is dependent in the bonding of the outer skin to the inner supporting grid. If the honeycomb is made to vibrate in a resonant mode and a 'time-averaged' holography taken, the discontinuities in the overall resonant fringe pattern directly gives the location of the subsurface faults.

USE OF LASER SPECKLES TO MEASURE DISTORTIONS

Another phenomenon which is proving quite promising for NDT is that of laser-speckles. When a surface of an object is illuminated by a laser one sees phantom bright spots which dance and jump as the eye of the observer moves. In the early days these dancing speckles were considered a nuisance and techniques were evolved for getting rid of them. Now they are proving valuable for research.

Strangely enough, these speckles were actually observed by Raman in India as early as 1919, much before lasers were invented. He was interested in haloes that surround the sun and the moon when a thin cloud floats by (Fig.19). These haloes can also be produced by having (lycopodium) dust particles spread thinly on a glass plate and viewing a distant point source (Fig.20). When these haloes are carefully observed they show a dotted or speckled appearance. A single spherical (say) particle produces a diffraction pattern of circular rings (Fig.21). The size of the particle defines the size of the rings. These rings can therefore be used to measure the sizes of extremely small particles. If there are n identical particles, the pattern remains the same, only the intensity becomes n times. Let us consider the intensity at any point on the screen where a diffraction maximum occurs. Each particle scatters light and these light waves reach this point. These waves will have the same amplitude A (if the particles are of the same size) but the phases would be different as the waves have travelled different distances (or paths). The resultant amplitude and phase of the light wave at any point of the screen will be given by the vectorial addition of all the light waves from the various particles. Therefore the resultant amplitude can vary from 0 to nA . The 'speckles' or bright spots appear where the interference is constructive and there is no light where the interference is destructive. Raman first used these speckles to demonstrate Brownian motion - the phenomena in which small microscopic particles suspended in a liquid, move erratically due to irregular molecular bombardment. When the haloes are observed through a drop of dilute milk (which contains microscopic colloidal particles) the speckles jump about erratically displaying the Brownian motion of the diffracting particles.

This experiment demonstrates that by observing the speckles, information can be obtained about the disposition or distribution of the particles. If a surface is illuminated by a laser beam, the scattered beam for the different points on the surface form the 'speckles'. If we had the intensity and phases of each speckle the exact disposition of the surface can be calculated

by a straight forward Fourier Transformation. Unfortunately, when the speckles are photographed the phase information is lost and so the reconstruction presents many problems. But these are identical to those connected with the phase problem in x-ray crystallography. We shall not discuss these today. Fig. 22 shows how spark speckle photography can be used to study the distortion of a honeycomb panel, the structural integrity of an aircraft wing or the distortion around a simulated crack in a large pressure vessel.

EXO ELECTRONS

When a metal is heated, it emits electrons. This effect was first discovered by Edison. When the thermal energy supplied is greater than the work function- the energy necessary to extract the electrons from the surface - 'thermal electrons' are emitted. If light falls on a metal and the energy of the photon is greater than the work function 'photoelectrons' are emitted. If a very strong electric field is applied the electrons inside a metal can be extracted. Kramers in the early 1940's while investigating why geiger counters behaved erratically for sometime after fabrication, discovered that freshly prepared or machined metal emit electrons (exo electrons). The exact physical reason for this electron emission is not yet completely understood. Fig. 23a shows the exo electron emission for a crumpled Aluminium foil which has been later straightened. A photographic plate placed on the foil for one hour produces this image showing the electron emission from the crumples and cracks. The exo electron emission lasts for a few weeks, being intense in the beginning and dying off slowly. This is well illustrated in Fig. 23b where numbers have been scribed on different days (month/day) using a mechanical vibrator on an aluminium foil. The picture shows the photographic plate after one hour exposure. The later writings are more intense than the earlier ones. Fig. 24 shows how the exo electron image can be intensified. A simple electrostatic lens focusses the exo electrons on to a multichannel electron multiplier plate with a gain of 10^7 . Individual electrons are converted to bright light spots of about $200 \mu\text{m}$ diameter: a magnification of 100 has so far been achieved. Melting, crystal transformations, plastic deformation, cracks and even incipient cracks emit exo electrons.

Exoelectrons are emitted spontaneously but they can be stimulated thermally or optically. By using ultraviolet light the exoelectron emission can be enhanced 10000 times. Instruments have been devised to scan a metal surface by an ultraviolet beam and study the exoelectron emission. Fig 25 shows an exoelectron image of a crack. It has been observed that when minute (incipient) cracks are formed due to fatigue, exoelectrons are emitted. When an object is subjected to fatigue even when it has undergone only 3% of its fatigue life exoelectrons reveal clearly where the material will fail! (Fig.26). This seems to be one of the most powerful tools for studying fatigue and fatigue life evaluation.

CONCLUSION

I have dealt with many topics and many fields- recent developments applied to many areas of research. One should not take this lecture to be a sales talk for importing of NDT instruments and techniques from abroad. Actually the purpose is exactly the reverse. I have also tried to show that basic discoveries in science can be used for the developments for extremely practical NDT techniques. I have also indicated that in some cases the discovery of the phenomenon was actually made in India but no development came out from here. This is where an organisation like HAL, if it is progressive and wise, can step in. It can promote real research and development. One wonders whether this seminar (which as far as I know is the first one to be held by HAL) is not the beginning.

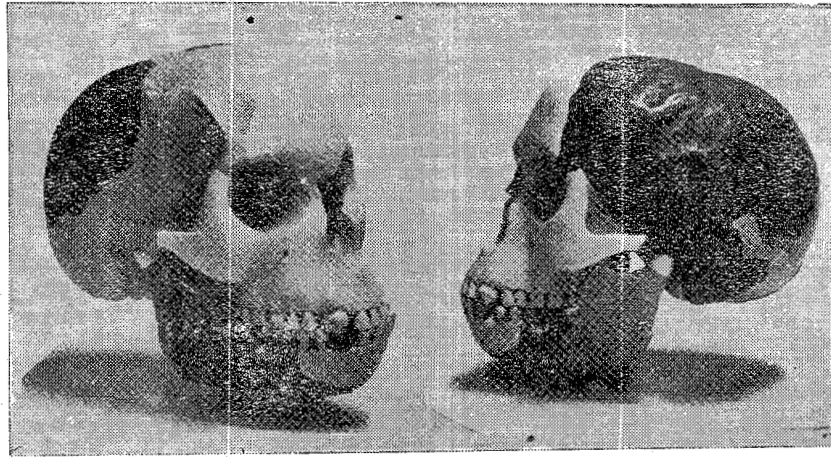


Fig. 1 Two views of the reconstructed skull of the 'Piltdown Man'

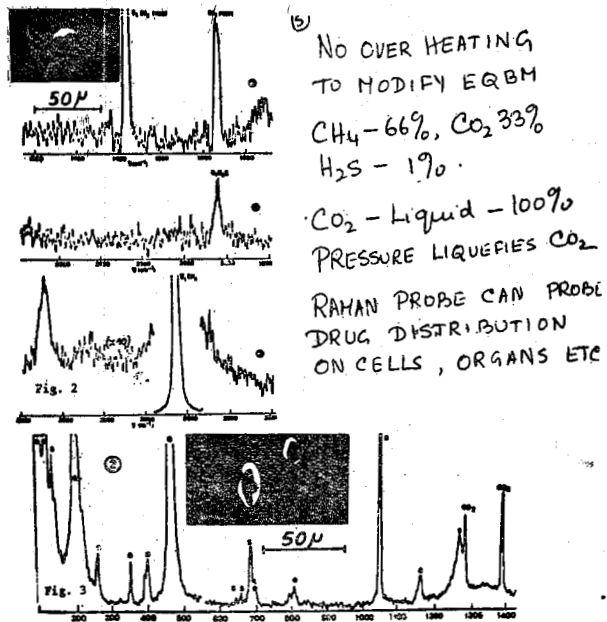
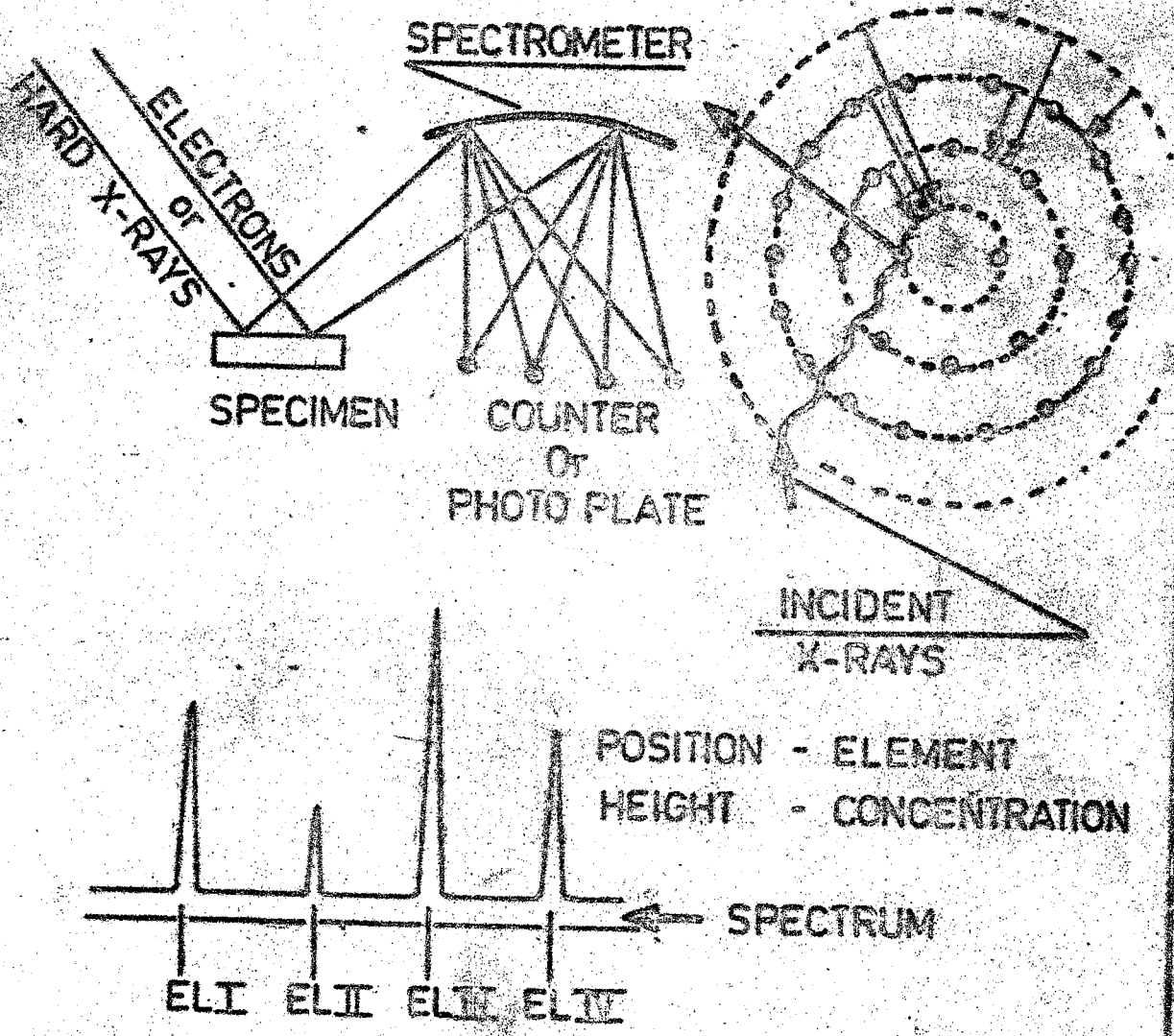


Fig. 4 Laser Raman Spectra of gaseous and liquid inclusions in minerals. The amount of material available is 10^{-9} to 10^{-10} gms. The first specimen has CO₂, CH₄ & H₂S. The second specimen contains pure liquid CO₂.



SPECTROMETER - WAVE LENGTH DISPERSIVE CRYSTAL
 Or
 ENERGY DISPERSIVE SEMI LIY

FIG 2. Principle of X-ray fluorescence analysis of elements.

LIQUID AND GAS INCLUSIONS IN MINERALS
 AMOUNT 10^{-9} - 10^{10} GRAM.
 MOLECULAR ANALYSIS ESSENTIAL.
 LASER RAMAN MICROPROBE ANALYSIS.
 VIBRATION FREQUENCIES ν_1, ν_2, ν_3

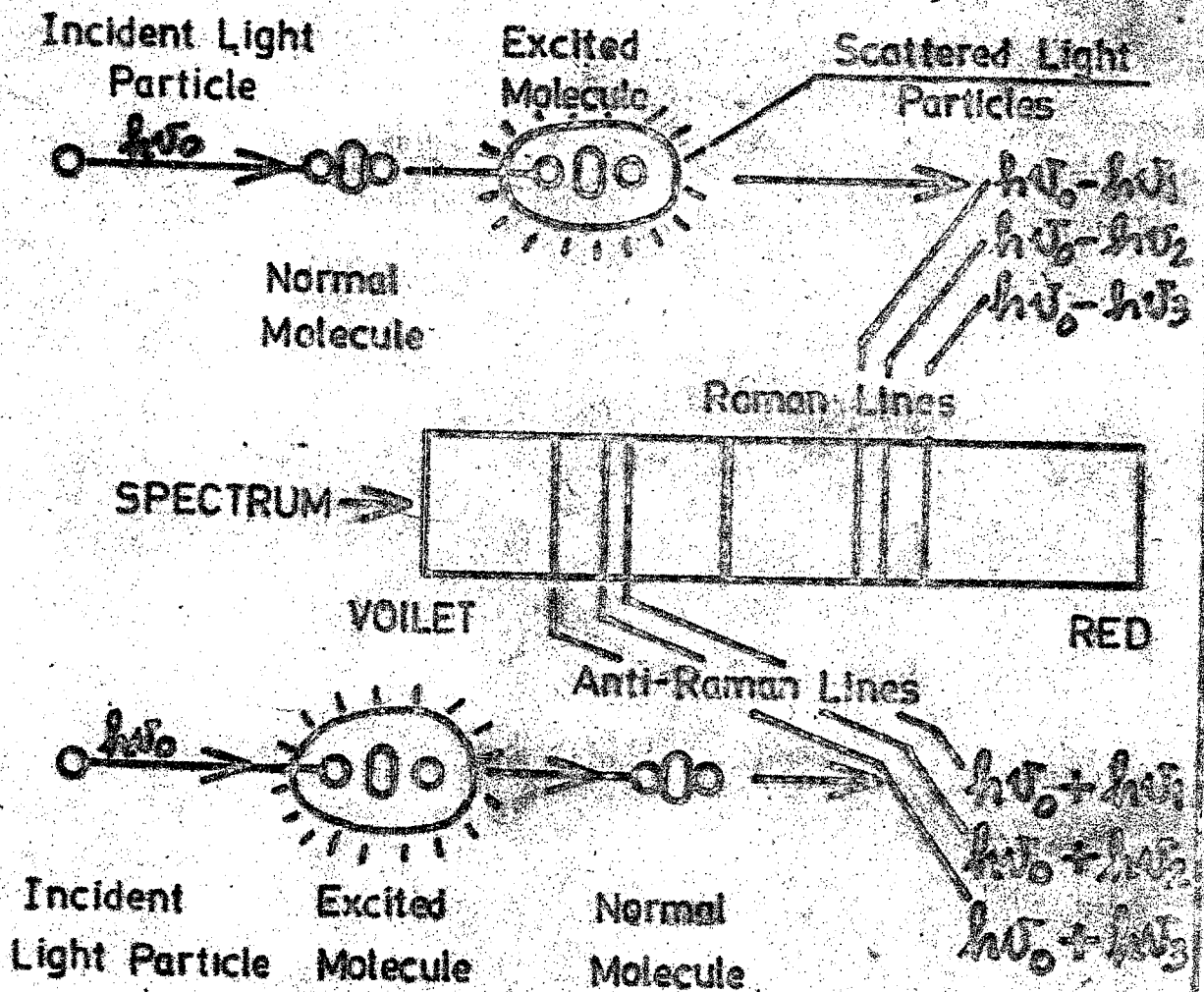


FIG 3. Principle of the Raman effect.

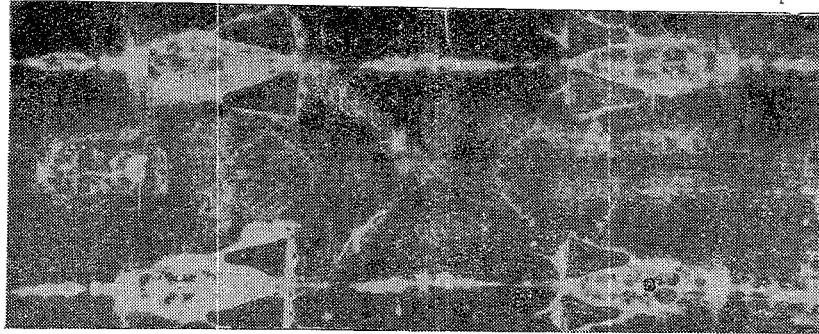


Fig. 5 The picture of the Turin Shroud. One theory is that the aloes and myrrh kept with the body made a chemical impression.



Fig. 6 A reconstruction by the 16th century artist Clovio showing how the body would have been wrapped in the cloth.

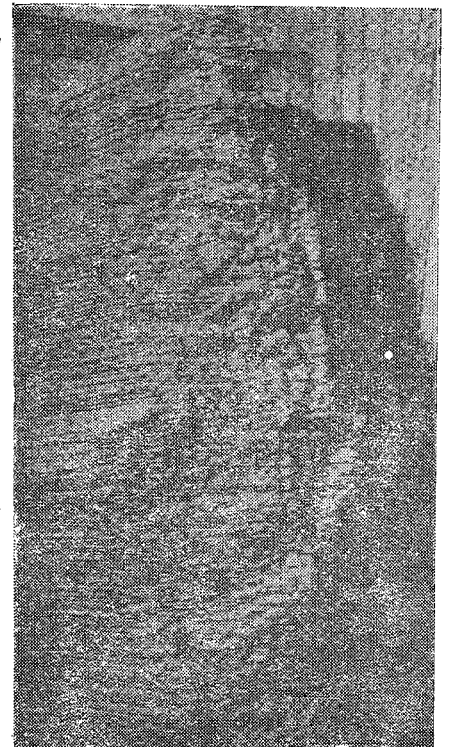


Fig. 7 A computer reconstruction of the figure assuming the darkening to be directly proportional to the distance of the shroud from parts of the body.



Fig. 8 X-Radiograph of human left hand taken by Rontgen.

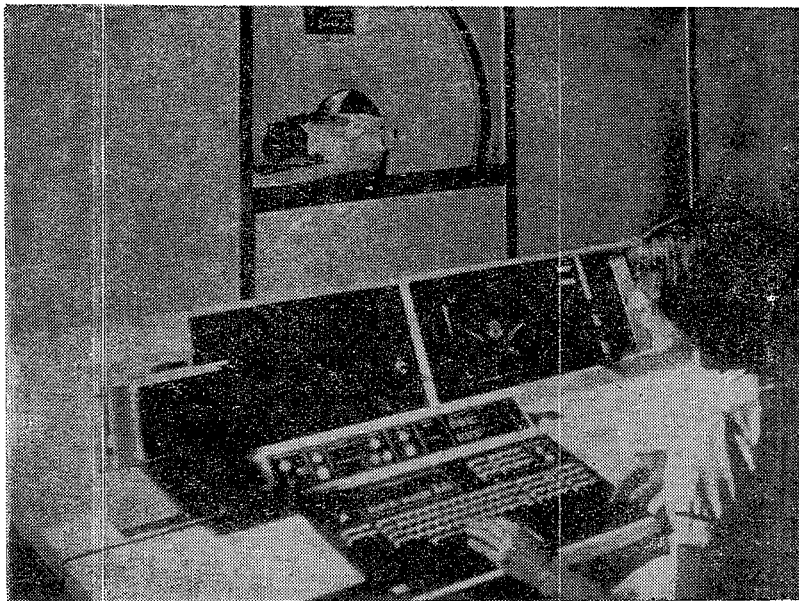


Fig. 9 X-Ray Tomographic machine.

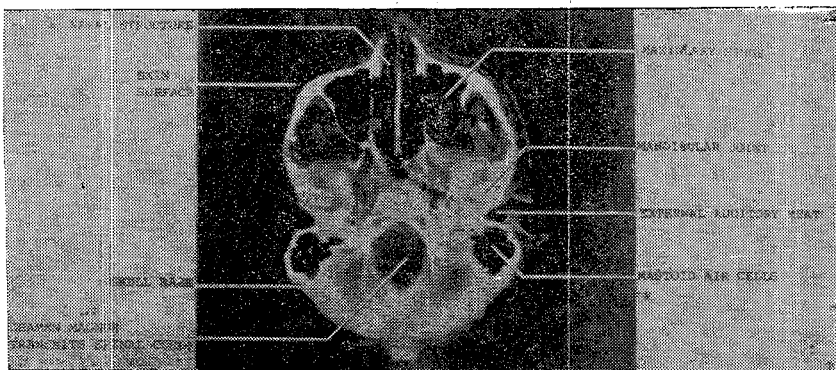


Fig. 10 X-Ray Tomograph of the human skull with an enormous amount of details.

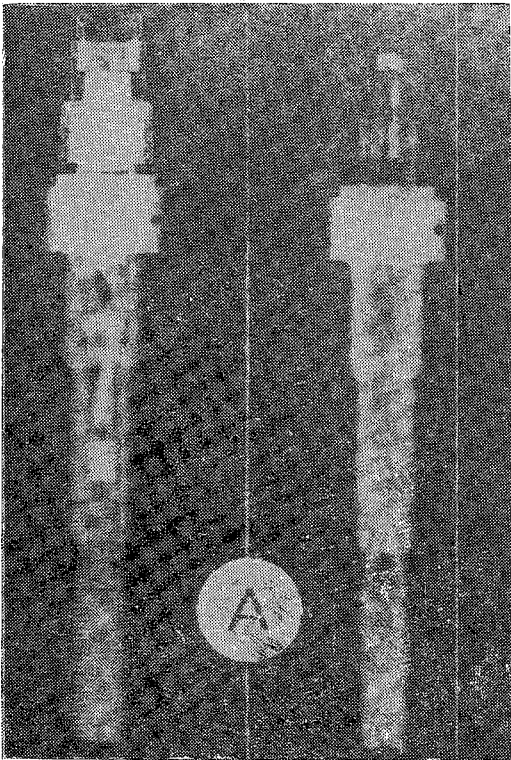


Fig. 11 Neutron and X-Radiograph of explosive pellet at the severance point to illustrate the complementary nature of the two. Neutron radiograph shows organic fill, plastic cap and coating. X-Radiograph shows the metallic components and lead based explosive.

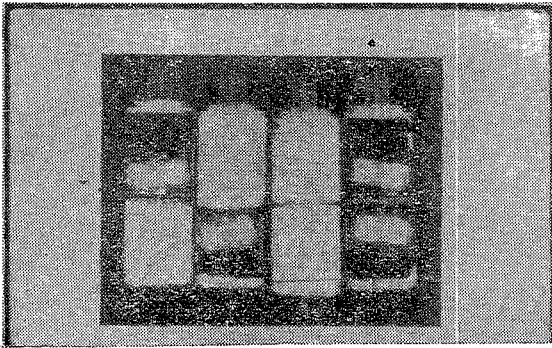


Fig. 12 Epoxy filled electronic filter. Some are filled completely and some having little or no epoxy potting.



Fig. 13 Neutron radiograph of epoxy bonded helicopter blade. Lack of epoxy is shown by the black areas. Non-uniform dark areas show a lack of epoxy due to the method of application and the extrusion of the epoxy.

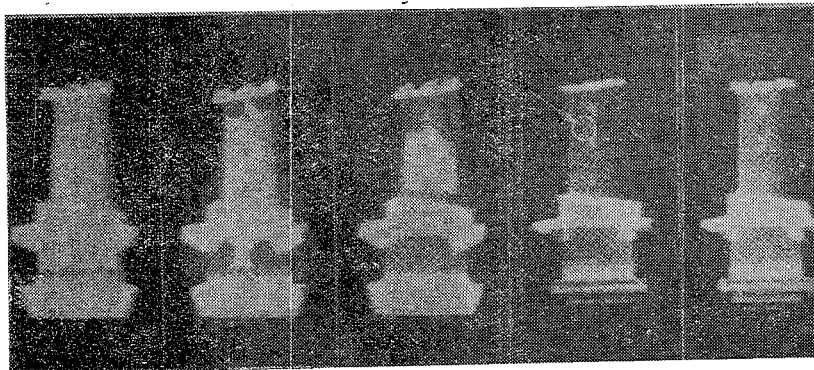


Fig. 14 Neutron Examination of ceramic core in turbine blades. Cd_2O_8 is added to make the ceramic opaque to neutrons.

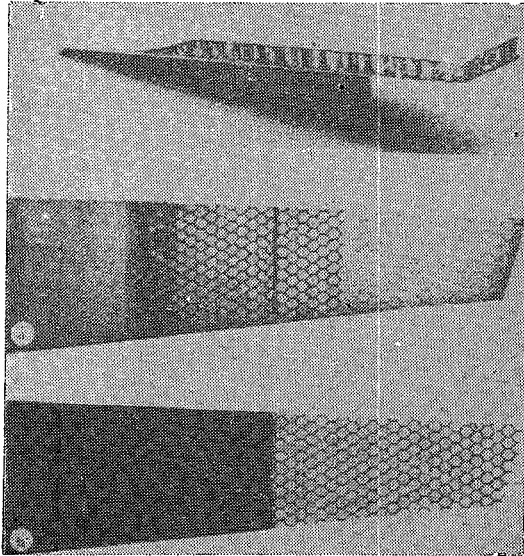
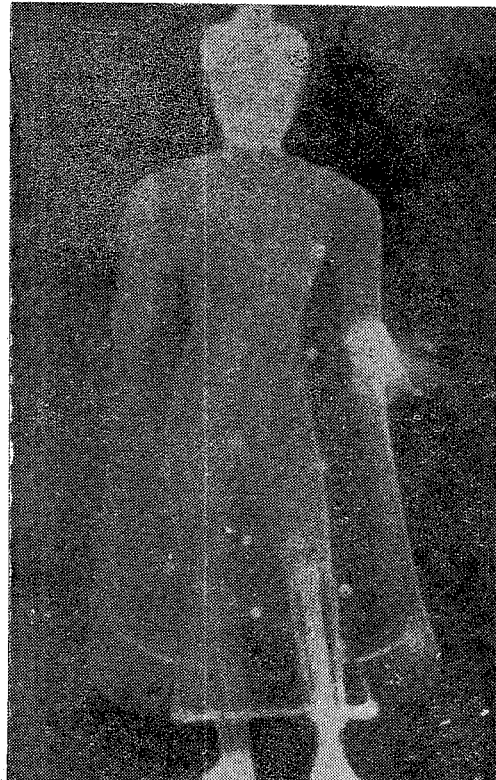


Fig. 15 Neutron and X-Radiographs of an epoxy bonded aluminium honeycomb specimen. The specimen (top of the figure) has a thickness of 0.425". The total thickness of aluminium facing sheet is 0.037". An additional aluminium stiffener (0.025") can also be seen. In the Neutron radiograph (centre) what appears to be the images of the aluminium case cell walls are actually absorption images of the cohesive fillings at the end of the core cell walls. X-radiograph of the same specimen (bottom) images only the aluminium stiffener plate (containing hole). The Neutron radiograph was obtained by using a 2 mg californium facility.

Fig. 16 Neutron Radiograph of a bronze statue cast in 800 AD. Clay cores are revealed and showed variations in the clay material (not shown by X-ray). Metallic pin in the clay core have been used to hold sections together. These pins are in the neck section to hold the head to the body during the bronze casting. The pins of different metal than the bronze are used in casting the statue. They show up very well (not visible in x-ray). One leg of the statue had been repaired in recent times. The Neutron radiograph showed that the hollow section of the broken leg has been filled with glue and a metallic wood screw was used to hold the two pieces together. X-rays showed the screws but not the glue.



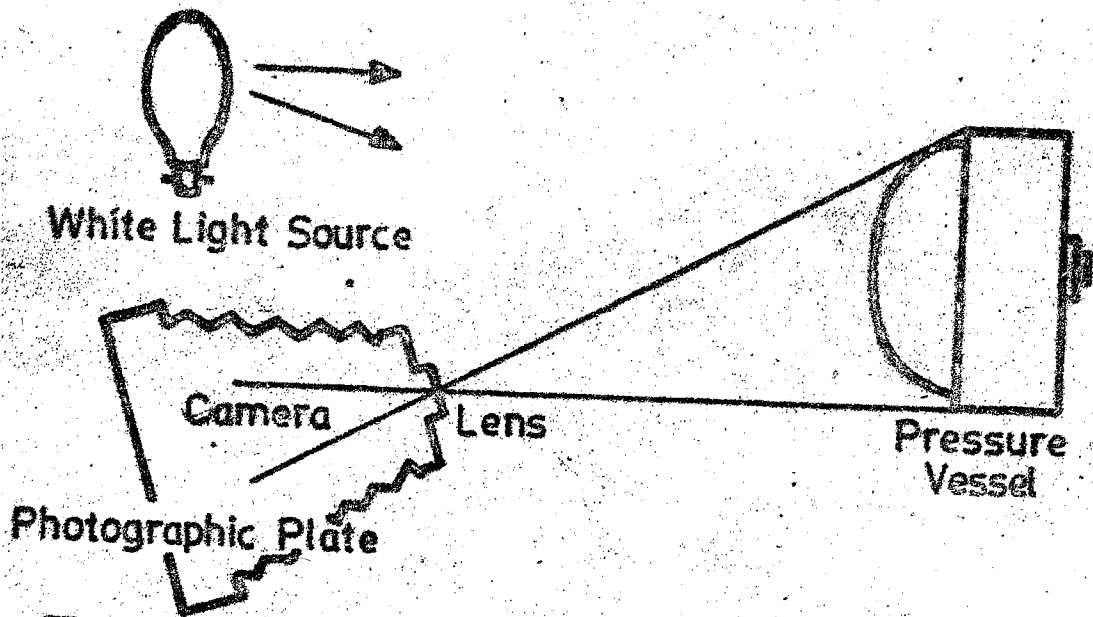


FIG 17a. Optical arrangement in two dimensional photography .

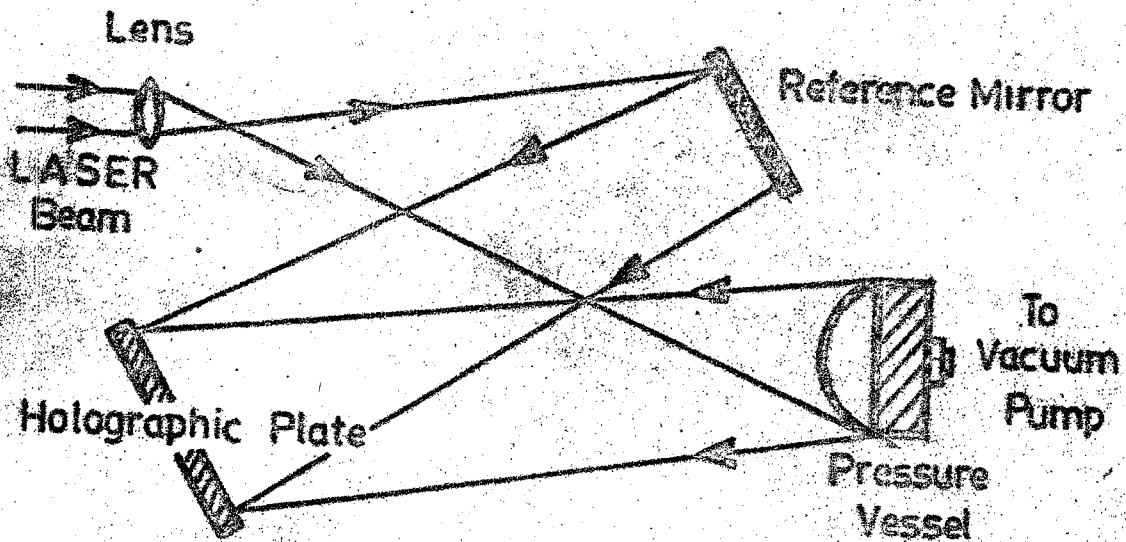


FIG 17b. Optical arrangement to produce a holograph .

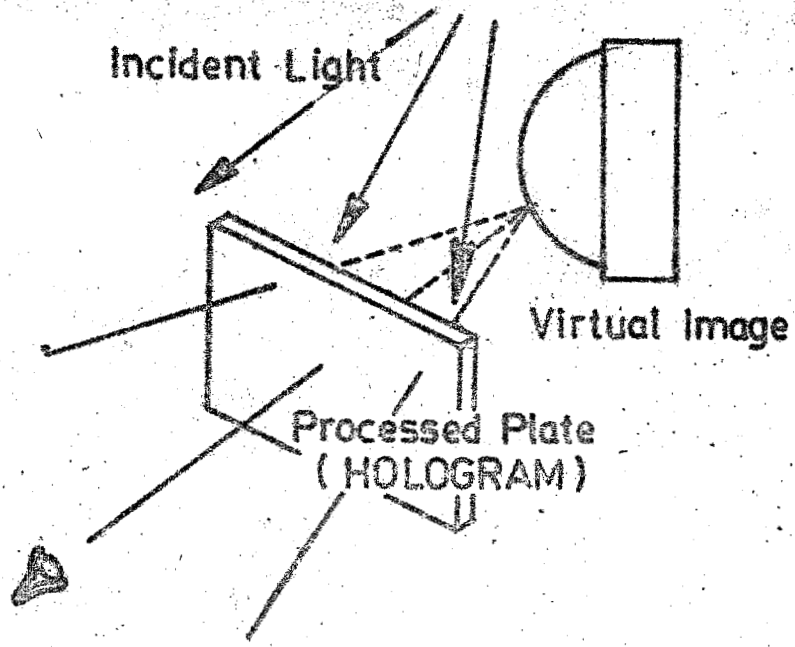


FIG 17c. Optical arrangement for holographic reconstruction.

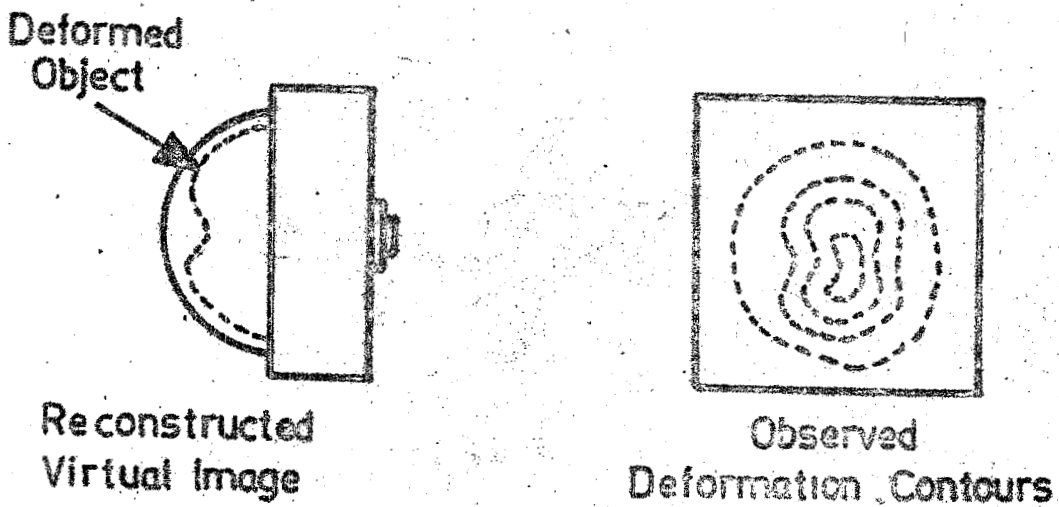


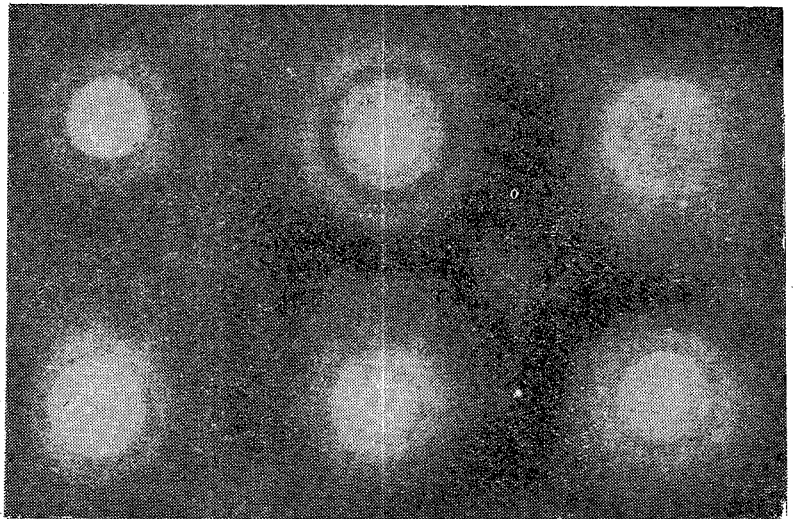
FIG 18a. Deformation contours.

Fig. 18b Holography used to examine crack propogation. A fatigue crack was formed at the end of a slot. With loading, plastic deformation occurs in a region surrounding the crack tip. The large deformation in this area can be seen in the photograph.



Fig. 18c Time averaged holography is used for flaw detection where the location of faults is found by noting the position of irregularities or discontinuities in the overall resonant fringe pattern. This is particularly useful to detect sub-surface faults. Picture shows the resonance fringe pattern of a honeycomb panel. Regions of 'disbonds' are clearly seen on fringe irregularities.

Fig. 19 Haloes due to water droplets similar to those seen around the moon or sun.



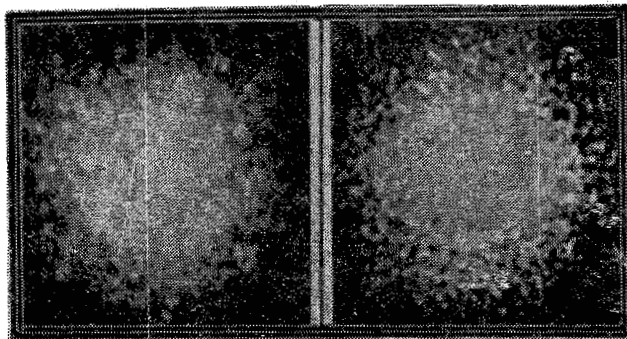
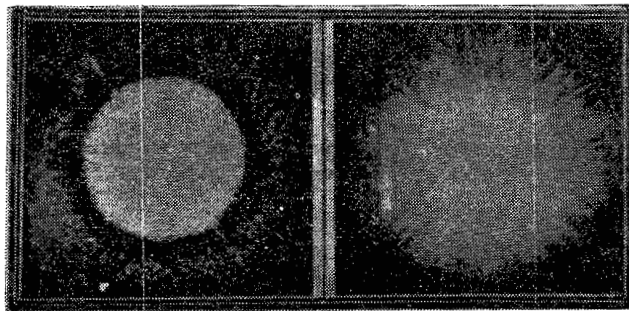
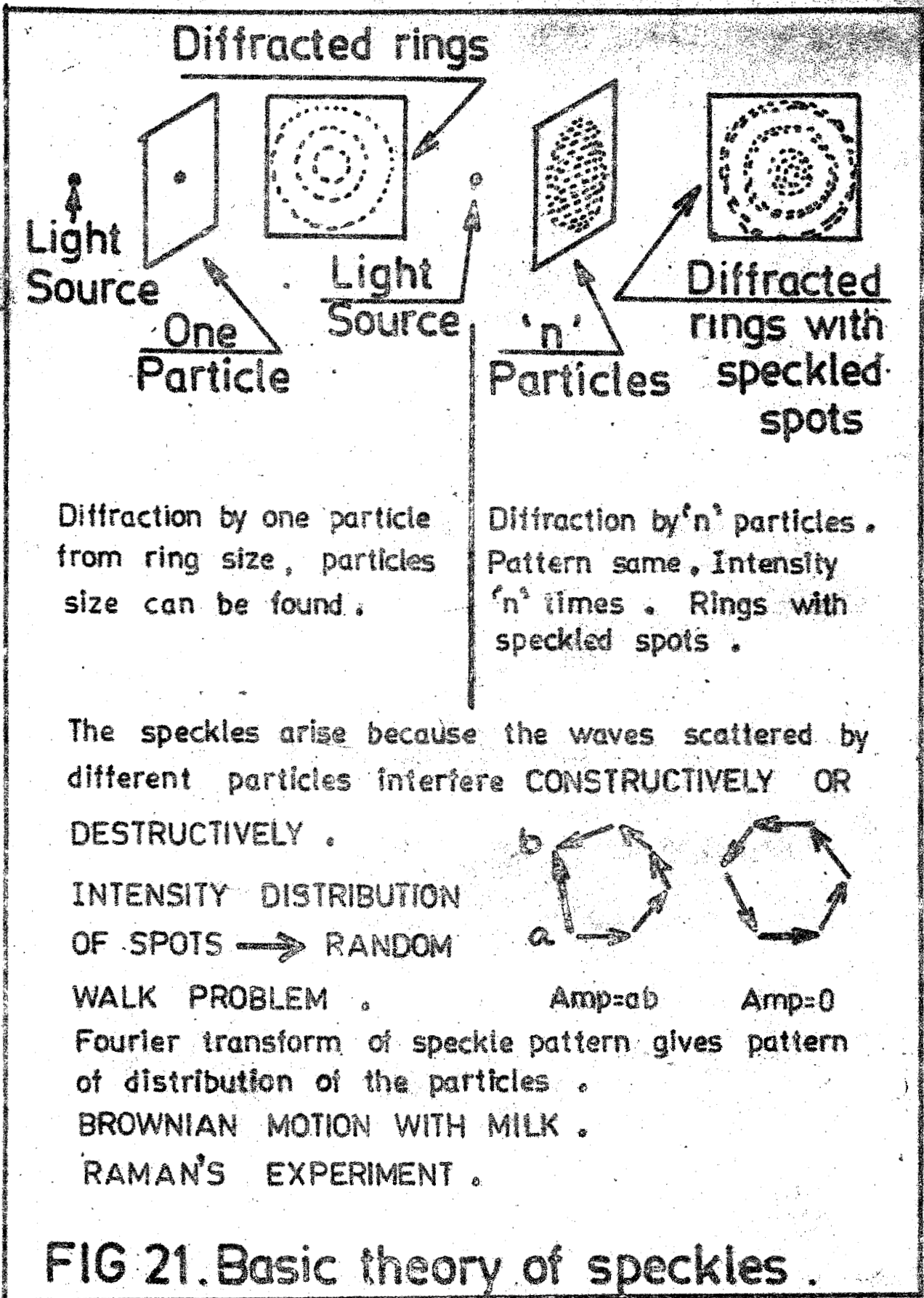
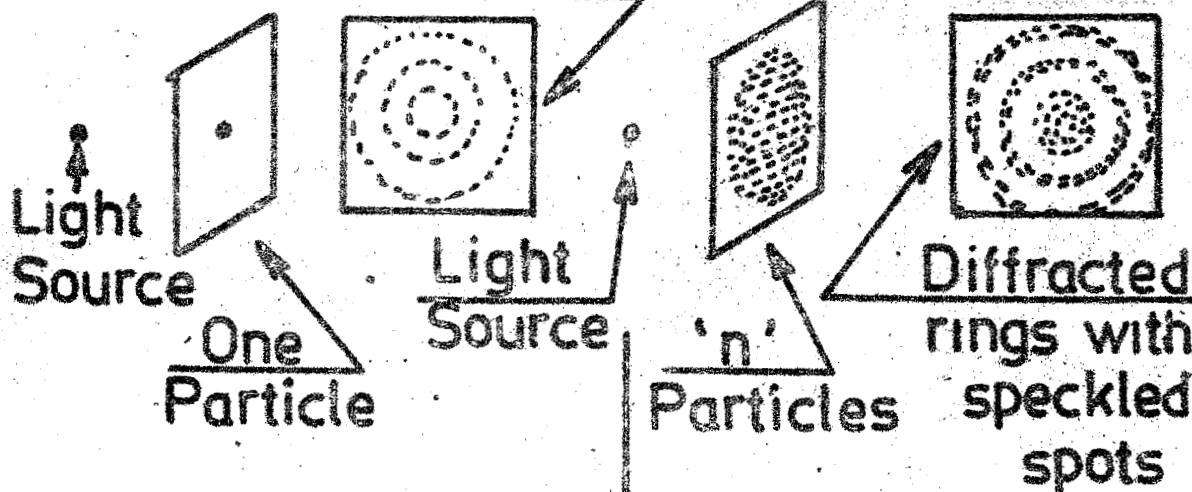


Fig. 20 Haloes formed by a lycopodium dust on a plate. Note the speckles in the haloes. These are actually images of the source. If the circular source is replaced by a triangular one, the speckles take a triangular shape.



Diffracted rings



Diffraction by one particle from ring size, particles size can be found.

Diffraction by 'n' particles. Pattern same, Intensity 'n' times. Rings with speckled spots.

The speckles arise because the waves scattered by different particles interfere CONSTRUCTIVELY OR DESTRUCTIVELY.

INTENSITY DISTRIBUTION OF SPOTS → RANDOM

WALK PROBLEM.



Amp=ab

Amp=0

Fourier transform of speckle pattern gives pattern of distribution of the particles.

BROWNIAN MOTION WITH MILK.

RAMAN'S EXPERIMENT.

FIG 21. Basic theory of speckles.

LASER SPECKLE PHOTOGRAPHY

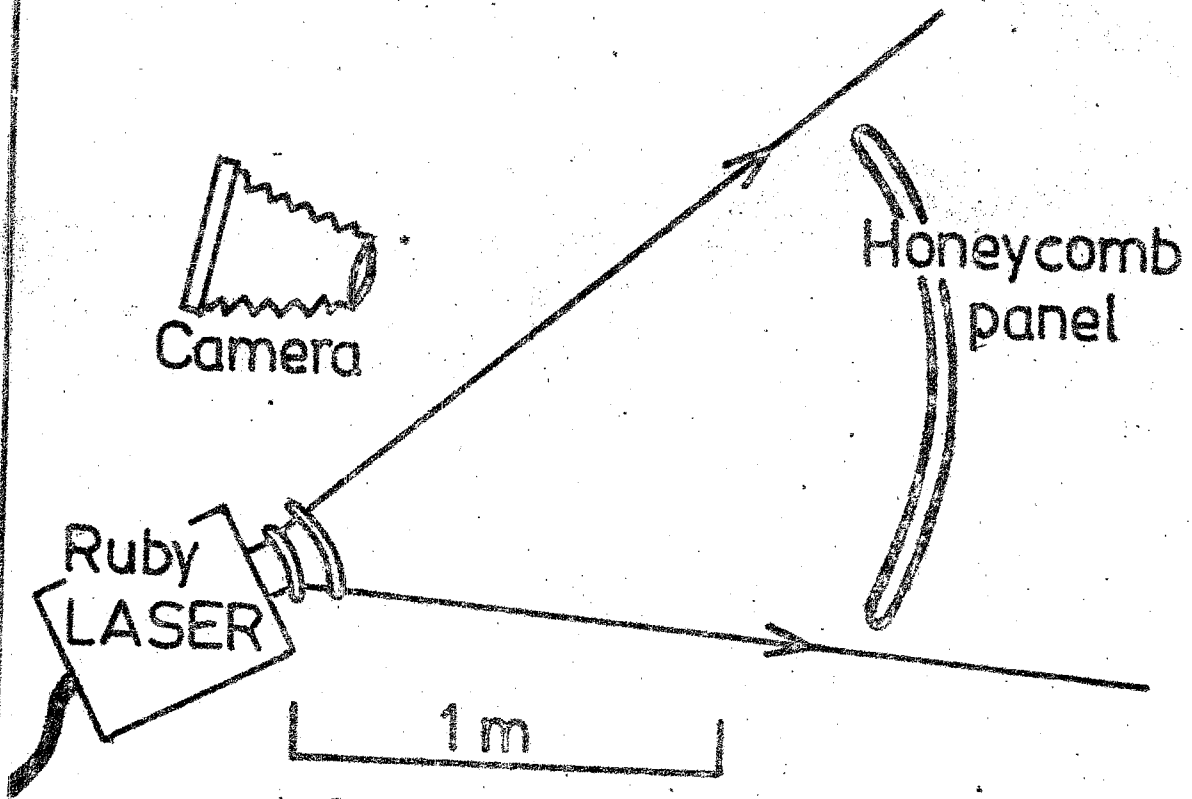
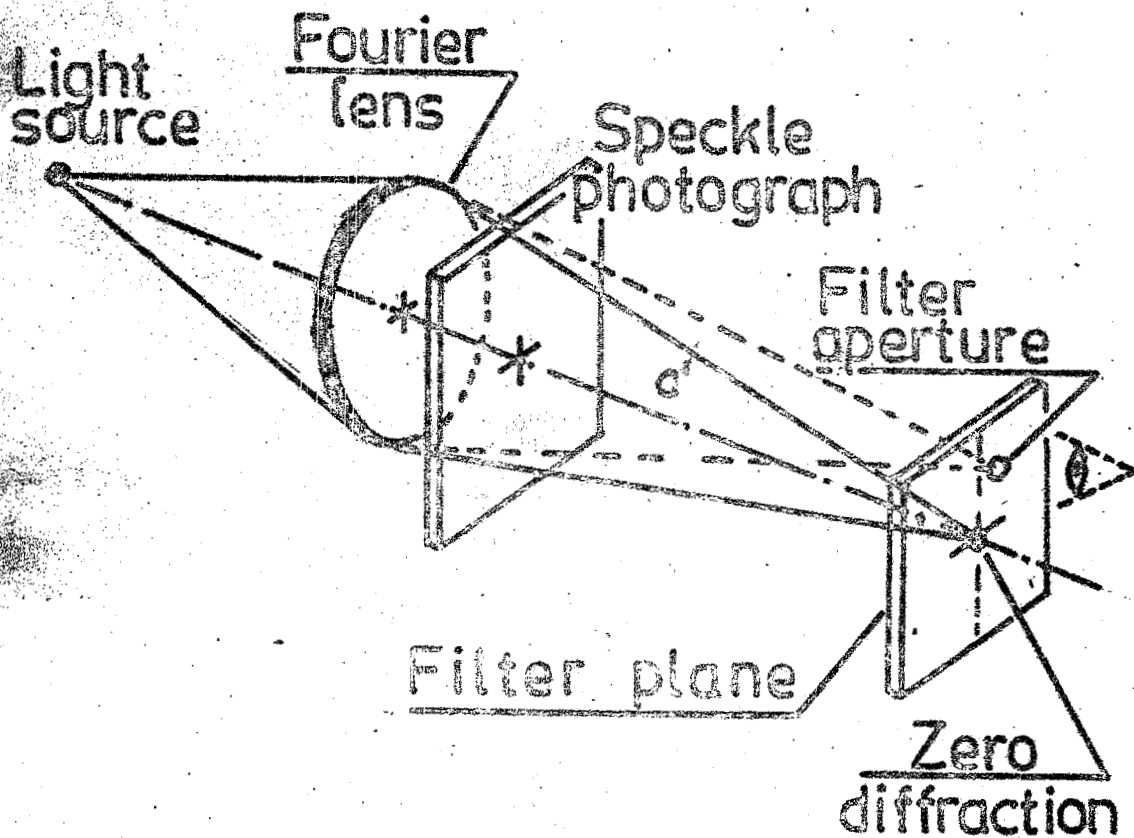


FIG 22a. Ruby laser speckle photograph with multiple emulsion camera to separate distortions.

LASER SPECKLE PHOTOGRAPHY.



Processing speckles.

FIG 22b. Fourier transform system for the analysis of defocussed speckle photography.

LASER SPECKLE PHOTOGRAPHY.

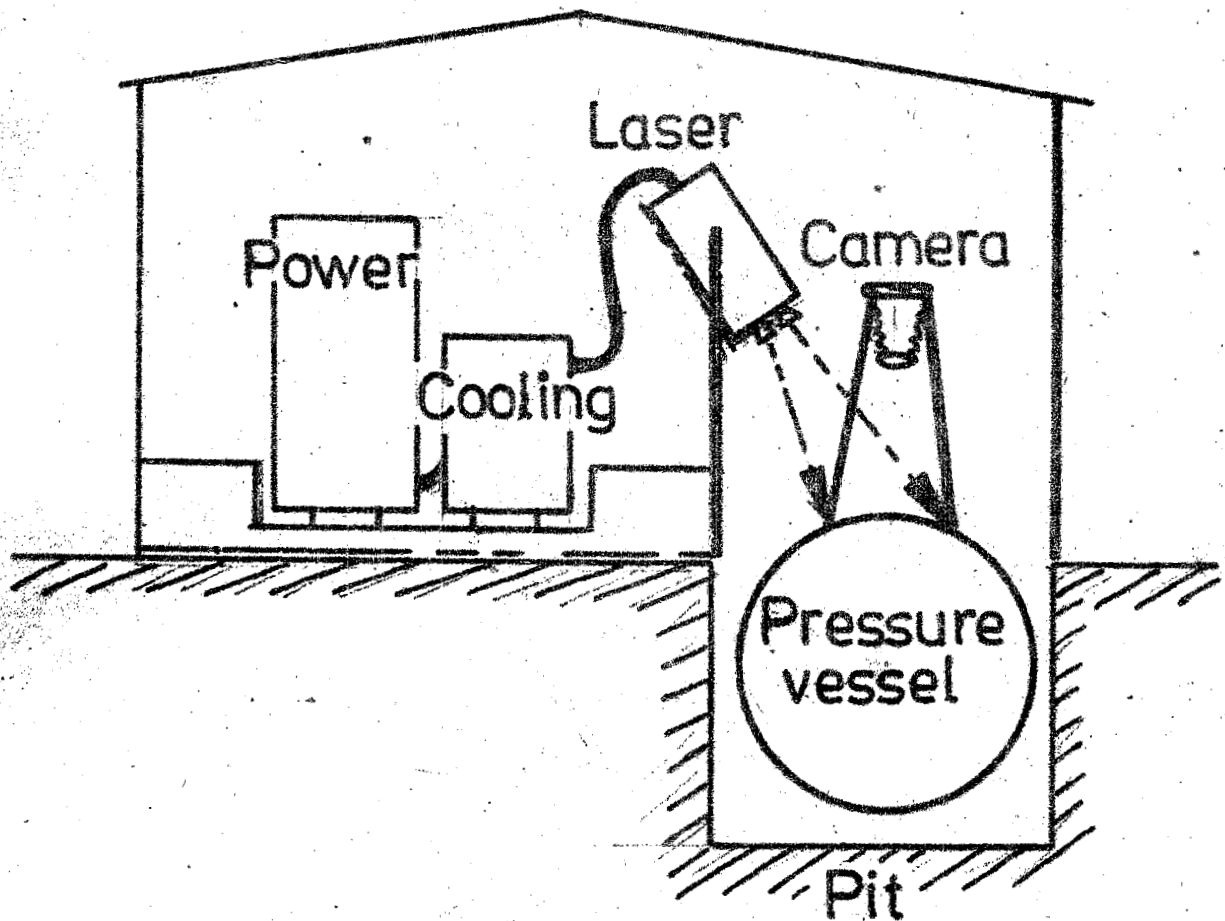


FIG 22c. Diagram for monitoring distortions around a simulated crack in a large pressure vessel using pulse laser speckle photography.

LASER SPECKLE PHOTOGRAPHY.

Aircraft wing

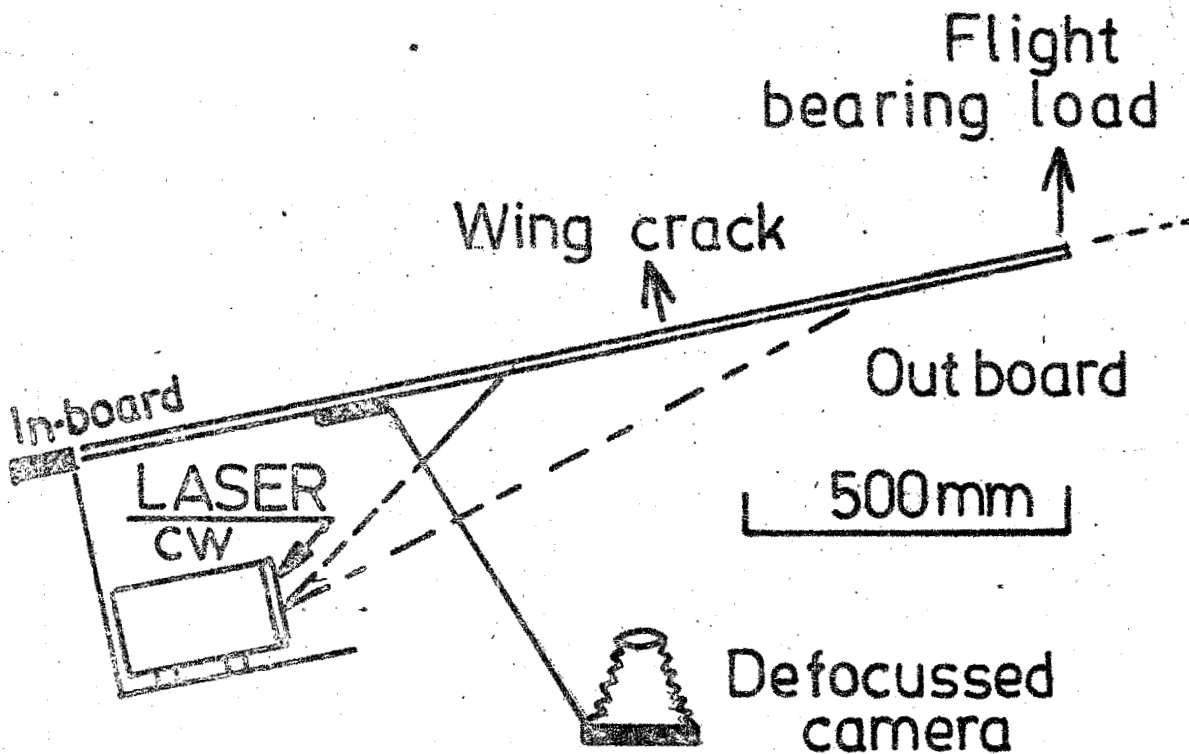


FIG 22d. Experimental arrangement for using speckle photography to study the structural integrity of an aircraft wing .

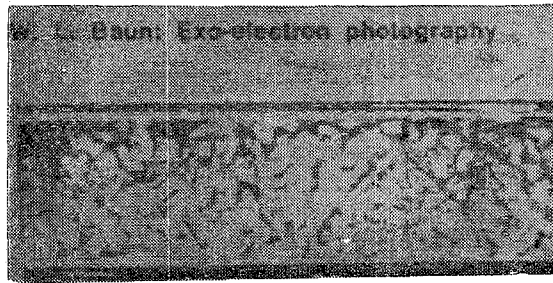


Fig. 23a Exo-electron emission from an Aluminium foil which has been crumpled and straightened. The picture is obtained by placing a photographic plate (with emulsion sensitive to electrons) on the foil for 1 hour.

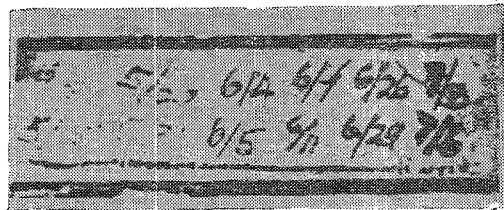
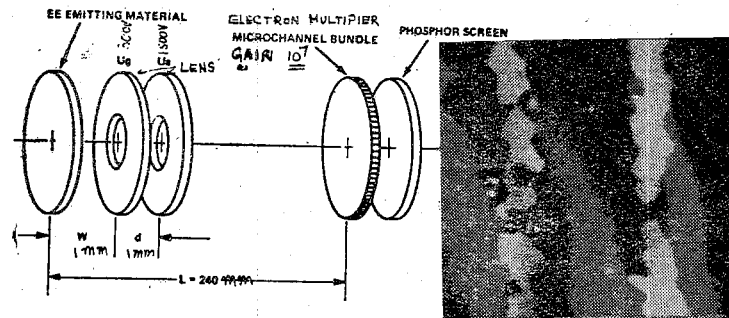


Fig. 23b Exo-electron emission from numbers scribed by a mechanical vibrator on different days on Aluminium foil (exposure 1 hour); the scribed numbers indicate the month and day of scribing. Note the numbers inscribed on later days are more intense.



EXO ELECTRON MICROSCOPE

Fig. 24 A simple exo- electron microscope and image

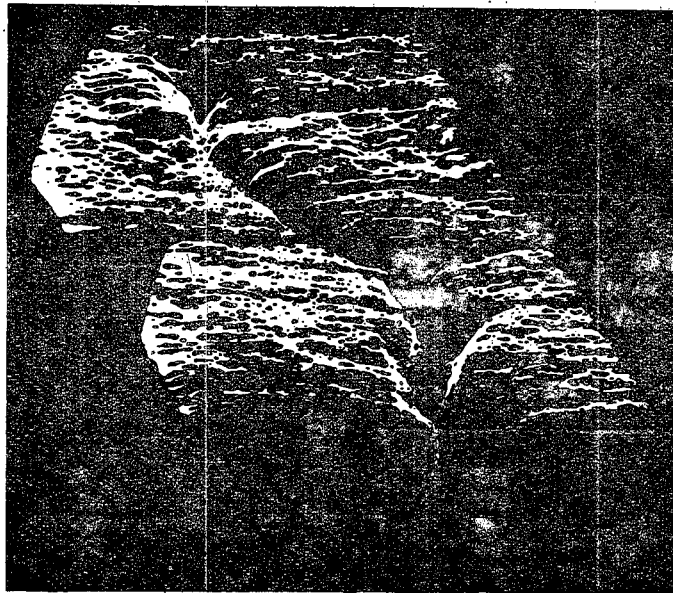


Fig. 25 An exo-electron image of a crack obtained by scanning the crack by a spot of ultraviolet light to enhance the exo-electron emission.

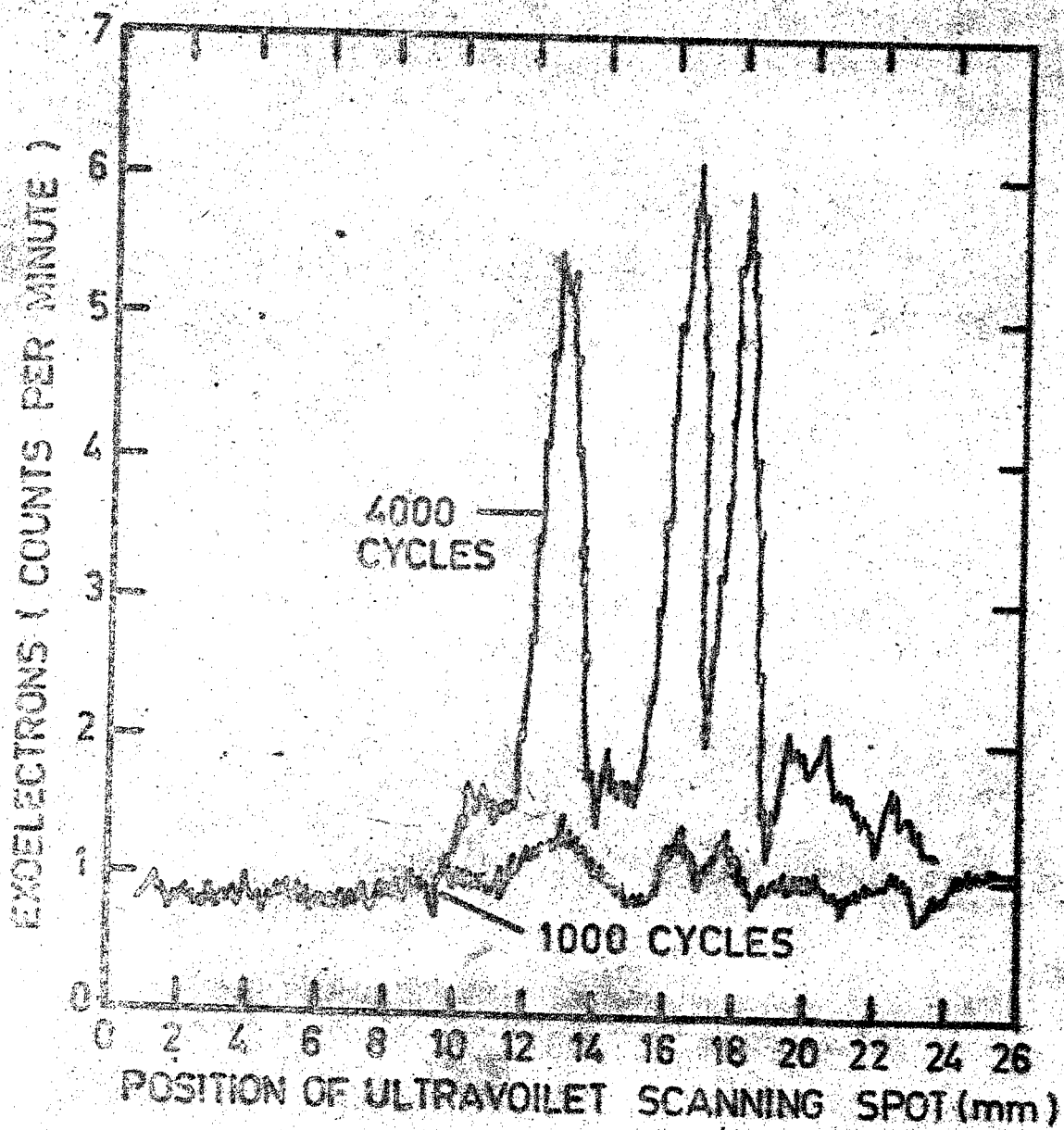


FIG 26. Emission of exoelectrons due to failure of the material due to fatigue.